Short Communication:

Adsorption of Methyl Orange Dyes on Oriented Co/Fe-MOF Bimetallic Organic Framework in Wastewater Treatment

Kim Ngan Thi Tran[1,2*], Cao Phuong Khanh Phan[3], Vuong Thinh Ho[3], Hung Dung Chau[1], and Thi Nhu Dung Nguyen[2,4]

[1]*Institute of Applied Technology and Sustainable Development, Nguyen Tat Thanh University, Ho Chi Minh City 70000, Vietnam*

[2]*Faculty of Environmental and Food Engineering, Nguyen Tat Thanh University, Ho Chi Minh City 70000, Vietnam*

[3]*Faculty of Chemical Engineering, Ho Chi Minh City University of Technology, Ho Chi Minh City 70000, Vietnam*

[4]*Ho Chi Minh City University of Natural Resources and Environment (HCMUNRE), Ho Chi Minh City 70000, Vietnam*

* ***Corresponding author:***

tel: +84-765712086
email: nganttk@ntt.edu.vn

Received: June 21, 2022
Accepted: August 23, 2022

DOI: 10.22146/ijc.75636

Abstract: *The production of highly efficient and reusable adsorbents that can be used in pigment treatment has been of great scientific interest. Metallic organic frameworks (MOFs) are considered a new type of material with extremely diverse structures and can be used as adsorbents to remove environmental pollutants. The selected Co/Fe-MOF material was synthesized in this study by using the solvent-thermal method. Then, the effects of several influencing factors such as adsorbent dosage, pH, initial concentration of MO, and exposure time on the adsorption capacity of methyl orange (MO) dyes by Co/Fe-MOF were evaluated. Under acidic conditions (pH 4), the effective removal of MO from aqueous solution reached equilibrium after 60 min upon exposure to MO at the concentration of 200 mg/L, and the adsorption capacity was 137.6 mg/g. The two models of adsorption isotherms, Freundlich and Langmuir, showed good compatibility with the experimental data, and the calculated correlation coefficients (R^2) were both greater than 0.96. The MO adsorption efficiency was proposed to fit the pseudo-quadratic and pseudo-first-order kinetic models. Therefore, MOF materials can be considered as a potential agent for wastewater treatment, thereby providing a possible solution to solve water pollution.*

Keywords: *bimetallic-organic framework; adsorption; methylene orange; kinetic model; isotherms model*

■ INTRODUCTION

In recent years, rapid industrialization development has been associated with the disposal of a large amount of wastewater and environmental pollution. One of the leading causes of environmental pollution has been widely known as textile dyes [1]. Previous studies have shown that direct disposal of untreated wastewater that contains toxic organic substances would significantly harm human health and destroy the natural environment [2-3]. Methyl orange (MO) is an anionic dye that is commonly used in the textile industry, with varied colors depending on the pH values. MO is recognized as a highly toxic substance and is associated with many health hazards [4].

Several methods have been used to remove chromogenic organic substances from aqueous media, such as precipitation, filtration, reverse osmosis, and adsorption. With the goal of achieving high efficiency at a reduced cost while reducing wastewater volume and improving the treatment quality, adsorption has been considered an effective method with numerous outstanding advantages [5-7]. Recently, the bimetallic organic framework (M/MOFs) containing the second metal (e.g., Ni, Co, Mn, and Cu) has much better adsorption capacity as compared with monometallic

materials [8-12]. The structure and properties of MOFs can vary depending on different ligands and metal ions, resulting in materials with high pore structure, large surface area, and multifunctional surface [13-14]. Therefore, MOFs have high applicability in the field of catalysis, gas storage, gas separation, adsorbent or electrode materials in sensors.

Recent studies have shown that the methylene blue removal efficiency of mixed MOFs was 2.8 times higher than that of Fe-MOF [15]. The Ni/Fe-MOFs became more porous, and the surface area was increased due to the formation of mixed metal clusters, as compared to the single-metal Fe-MOFs [16]. Wang et al. [17] successfully synthesized Ti-doped Fe-MOFs bimetallic materials to increase the yield and shorten the decomposition time of Orange II. In another study, MM−MOF was synthesized by replacing Fe^{3+} in Fe-BDC with Cu^{2+} to obtain FeCu-BDC. Significantly, the synergistic effect of Fe and Cu on the material surface as a heterogeneous catalyst was evaluated for the antimicrobial activity of sulfamethoxazole (SMX) [12].

Therefore, in order to promote the attractive properties and increase the adsorption capacity of MOF materials, the present study has combined Fe-MOF with Co^{2+} metal ions to prepare Co/Fe-MOF material based on the solvothermal method in *N*,*N*-dimethylformamide solvent with the combination of metal salts and 1,4-benzenedicarboxylic acid ligand. The MO dyes were used in this study to evaluate the adsorption capacity of the material.

■ EXPERIMENTAL SECTION

Materials

Chemicals and reagents used in this study were $FeCl_3{\cdot}6H_2O$ (99%), $Co(NO_3)_2{\cdot}6H_2O$ (99%), and 1,4-benzenedicarboxylic acid (99.8%) from Xilong-China. Meanwhile, *N*,*N*-dimethylformamide (DMF) was purchased from Macron-Fisher and methyl orange dye was obtained from Sigma-Aldrich.

Instrumentation

Equipment used in this study included a Memmert UN110 oven (108 L, 300 °C), a thermostatic shaker Jeotech IST–4075 (20 erlen, 250–300 mL), a Teflon-lined solvothermal synthesis autoclave reactor (100 mL), 8D Advance Bruker (Germany) for XRD, Nicolet 6700 device-Thermo Fisher Scientific (USA) for FTIR, S4800-JEOL Japan for SEM, Micromeritics 2020 (USA) for BET, and UV-Vis spectrophotometer (Thermo, USA).

Procedure

Synthesis of Co/Fe-MOF sample

The Co-doped Fe-MOF material was synthesized through the solvent-thermal method, following the previous protocol by Ding et al. [18] with slight modifications. At first, $FeCl_3{\cdot}6H_2O$ (99%) and $Co(NO_3)_2{\cdot}6H_2O$ were mixed at a mass ratio of Co^{2+}:Fe^{3+} of 0.267 and 2.482 g. Subsequently, 0.83 g of 1,4-benzenedicarboxylic acid was dissolved in 60 mL of DMF under constant stirring for 30 min. The solution was allowed to react at 150 °C for 20 h in a 100 mL Teflon tube with a stainless steel-based protective case. The mixture was then allowed to cool reaching room temperature, centrifuged to separate the solids, and washed with DMF and ethanol. The synthesized material was then vacuum dried at 120 °C for 24 h.

Characterization of the synthesized materials

The physical properties and structural composition of the were analyzed by several methods. X-Ray Diffraction (XRD) was measured by using Cu-Kα radiation at 2θ scanning angle from 10 to 35°. The characteristic functional groups on the surface of materials through FTIR spectroscopy. The structure and crystal morphology of the materials were analyzed by SEM images. The surface area and porosity of the adsorbent were determined by N_2 adsorption-desorption isotherm (BET). The MO adsorption capacity of the materials was determined using a UV-Vis spectrophotometer.

Methyl orange (MO) adsorption experiments

The adsorption capacity of the MO-removing materials was evaluated based on several influencing factors such as contact time, pH, adsorbent dosage, and initial MO concentration. The adsorption was carried out in a 250 mL conical flask and placed on a heat shaker at 200 rpm. In each experiment, adsorbent at various concentrations of 0.002–0.030 g/L was accurately

weighed and mixed with 50 mL of MO solution (concentrations ranged from 30 to 300 ppm). The pH factor of the medium was also adjusted within the range of 2–12. After 10 to 240 min, 4 mL of sample solution was removed and centrifuged at 6000 rpm for 5 min to separate the adsorbent. The concentration of MO dye was determined at λ_{max} = 465 nm on a UV-Vis instrument.

■ RESULTS AND DISCUSSION

The structural characteristics and crystalline phase composition of the synthesized materials were determined based on the results of the XRD analysis. Fig. 1(a) has shown that Fe-MOF and CoFe-MOF samples have characteristic diffraction peaks appearing at 2θ angle < 30°, which are the characteristic diffraction peaks for Fe-MOF. It is significant to be noted that the positions of XRD diffraction peaks of these CoFe-MOF materials have a slight shift towards the smaller 2θ angle than that of the synthesized Fe-MOF under the same conditions, indicating that Co has been phased doped into the Fe-MOF lattice. Blake et al. [19] firstly explained that the partial replacement of Fe^{3+} ions with other divalent metal ions (M^{2+}) would lead to a slight decrease in the Fe–O bond length and a slight increase in the Fe–O–Fe angle. The process of doping Co in Fe-MOF causes the diffraction intensity to decrease but still maintains the Fe-MOF structure. In addition, the ionic charge significantly affects the material modification efficiency. Competition for electron affinity between two metal ions with the same charge leads to distortion of the original material structure [20].

The FTIR spectra of Fe-MOF and CoFe-MOF samples show that the sample has a full range of material-specific oscillations at the absorption bands at 532, 751, 1390, 1589 and 3600–3000 cm^{-1}, respectively (Fig. 1(b)). The symmetric and asymmetrical elongation of O–C–O is shown by oscillations in the region 1600–1400 cm^{-1}. Fe-O oscillations and C-H bending vibrations of benzene are located at the maximum peaks of 532 and 751 cm^{-1}, respectively. In addition, the formation of bimetallic centers of CoFe-MOF was determined based on the clear appearance of the peak at 622 cm^{-1}, corresponding to the Co-O oscillations. This result is in high agreement with the previous study by Liang et al. [21].

The surface morphology of the material was determined by SEM images, and the results are presented in Fig. 2. The results show a clear change in the shape and size of the material in the presence of Co^{2+}. In the Fe-MOF sample, the surface morphology is uneven, the particle size is large, the grain boundary is not clear, and there is a clump of particles. When doping Co^{2+} ions into the Fe-MOF lattice framework occurs, the particles are uniform in size and shape. The grain size is more obvious, and the catch shape tends to have sharp peaks. The ratio difference in the reaction between Fe^{3+} and Co^{2+} with H_2BDC facilitates the growth of bimetallic MOFs.

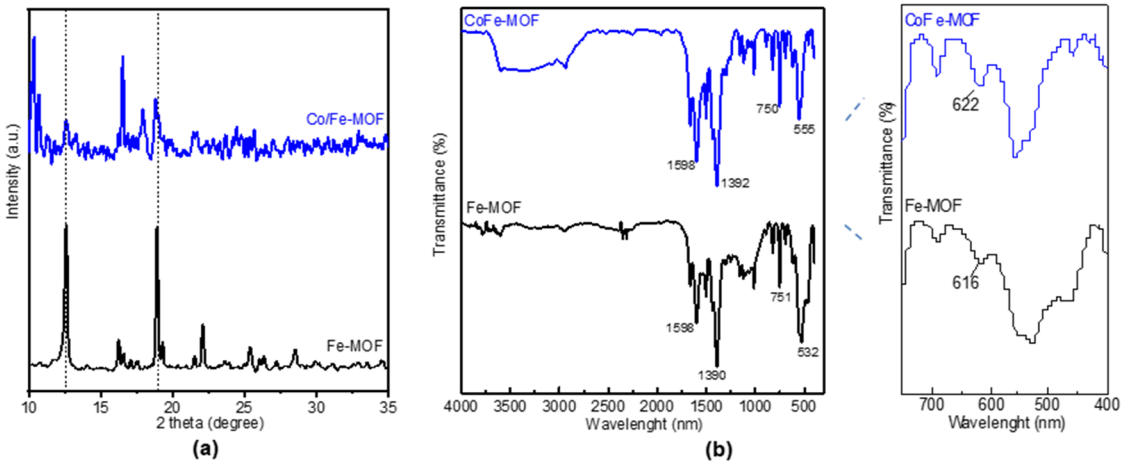

Fig 1. XRD patterns (a) and FTIR spectra (b) of Fe-MOF, CoFe-MOF

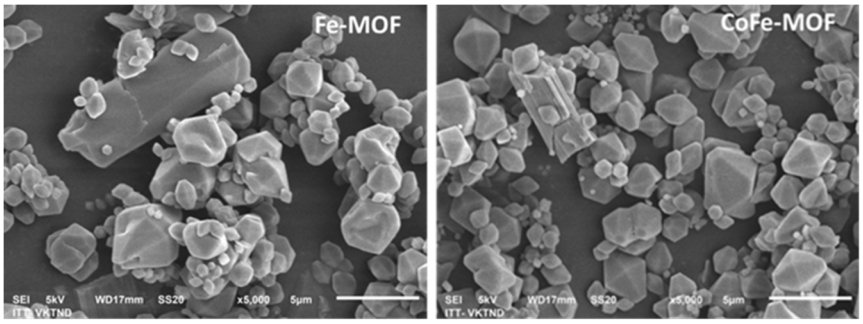

Fig 2. SEM image of the as-synthesized MOF

The N_2 adsorption and desorption isotherms of the composites are shown in Fig. 3. The results show that the isotherm curve belongs to type II, according to the IUPAC classification. The synthesized Fe-MOF and CoFe-MOF materials have a BET surface area of 32.8 and 52.6 $m^2.g^{-1}$ and pore volumes of 0.06 and 0.09 cm^3/g, respectively. The presence of Co metal in the Fe-MOF framework increases the specific surface area and porous volume, thus increasing the accessibility of the active sites and molecular diffusion to facilitate the high adsorption efficiency of water pollutants [22]. The inclusion of the second metal in the Fe-MOF framework is beneficial to promoting complete contact of the active sites of the resulting bimetallic M/Fe-MOF. The modification of metal ions into the original structure will contribute to the release of charges, making the material more porous and increasing the surface area. Recent research by Wang et al. [23] showed an increase in specific surface area in the presence of the second metal Co at different ratios with Fe-MOF (32.8 $m^2.g^{-1}$) and FeCo-MOF-1/3 (466.3 $m^2.g^{-1}$). The presence of Co metal in the Fe-MOF framework increases the specific surface area and porous volume because the Co radius (65 nm) is slightly larger than that of Fe (64 nm), and the carboxyl groups react simultaneously with two metal ions.

One of the important parameters that directly affect the adsorption process is pH. Fig. 4(a) shows that the MO adsorption capacity of CoFe-MOF is higher than that of Fe-MOF in the pH range from 2 to 12. The MO adsorption capacity of the materials increases continuously from pH 2 to 4, yet sharply decreases when pH continues to increase to 12. The highest MO adsorption capacity of CoFe-MOF (104 mg/g) was achieved in an acid medium at pH 4. Therefore, it can be seen that the adsorption

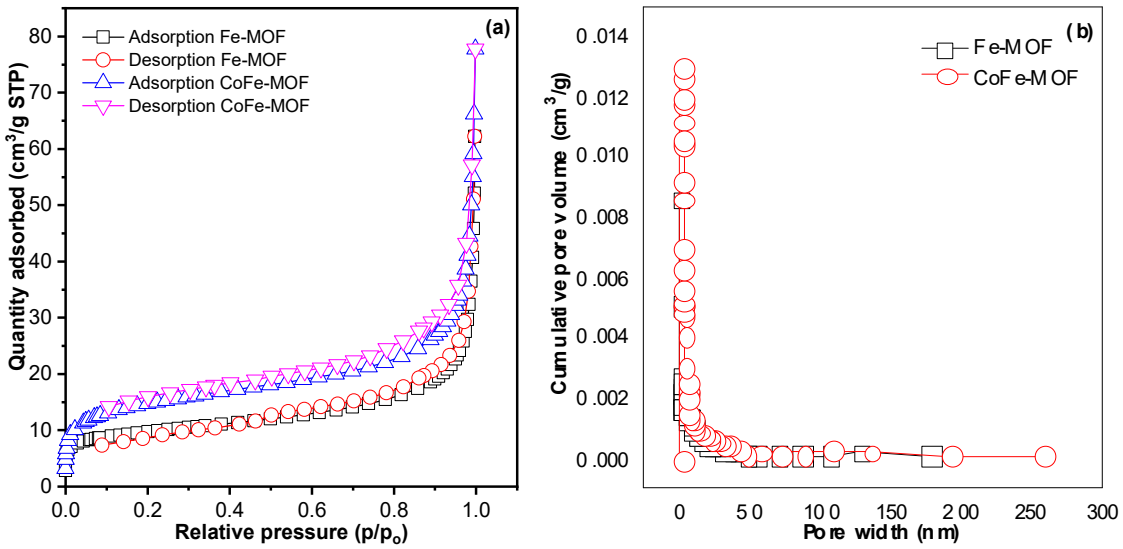

Fig 3. N_2 adsorption-desorption isotherms (a) and pore size distributions (b) of Fe-MOF and CoFe-MOF samples

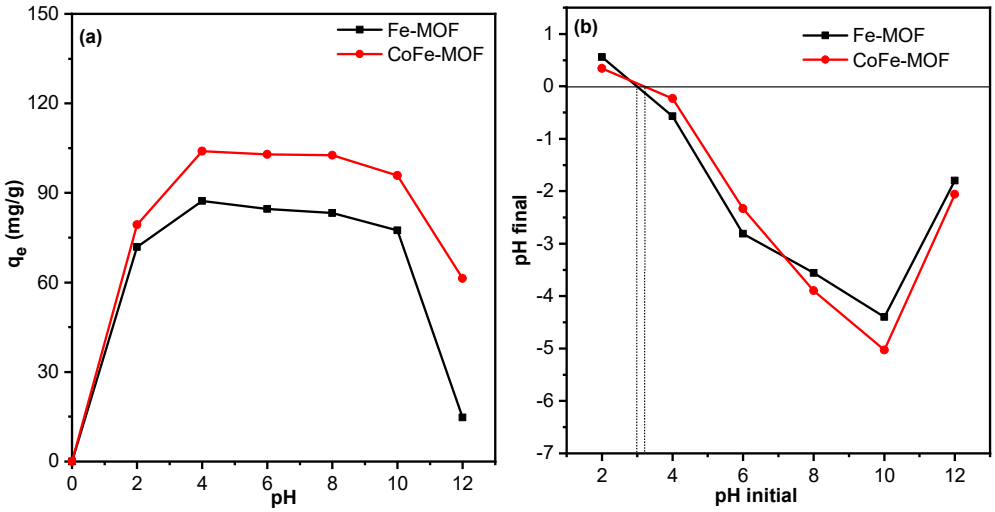

Fig 4. Effect of initial pH MO (a) and zero charge point (b) of Fe-MOF and CoFe-MOF

capacity of both materials strongly depends on the pH value. Furthermore, the surface charge of the adsorbent is also an important factor that requires attention. The surface charge of the material is evaluated based on the pH_{pzc} parameter when the pH variation reaches zero. Fig. 4(b) shows that the pH_{pzc} values of Fe-MOF and CoFe-MOF are 3.0 and 3.2, respectively. With the value of pH_{pzc} < pH, it is possible to determine the surface of the material exhibits a negative charge, which corresponds to the previous study [24]. The doped metals reduce the specific surface area of Fe-MOF, and the changes in the crystal structure and appearance morphology mainly produce the enhancement of adsorption capacity, which is due to competitive coordination between metal ions doped with saturated iron ions to bind carboxylic groups in the BDC and thus an increasing number of active Fe sites are generated.

Subsequently, the effect of time, the dose of adsorbent, and the initial concentration of MO on the removal of MO colorant in an aqueous solution by Fe-MOF and CoFe-MOF samples were then investigated. For the effect of time, the adsorption reached equilibrium within 240 min under the conditions of fixed pH, adsorbent dosage, and initial MO concentration (Fig. 5(a)). The MO adsorption capacity of CoFe-MOF took place quickly within 60 min with an adsorption capacity of 105.2 mg/g. In contrast, the adsorption capacity of Fe-MOF material only reached

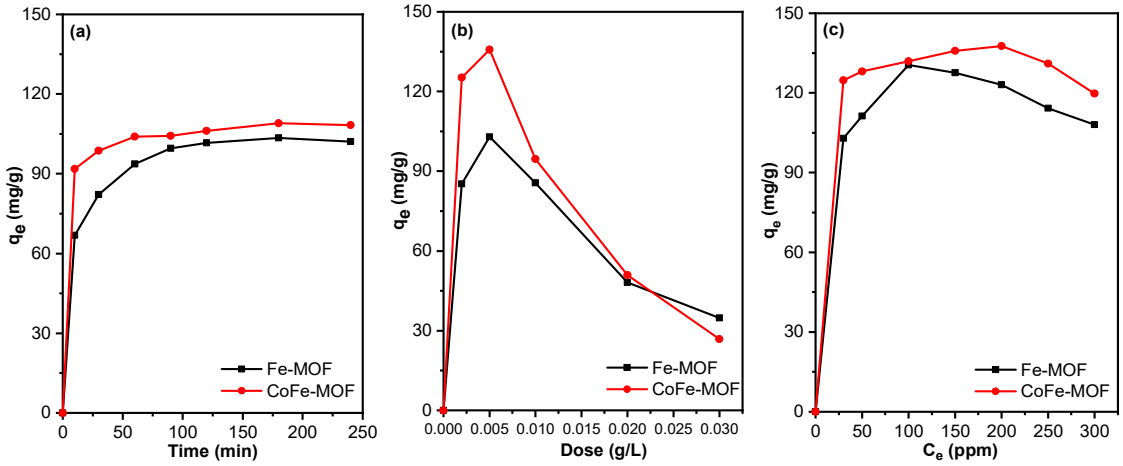

Fig 5. Effect of time (a), dose (b) and MO concentration initial (c) on the adsorption capacity of Fe-MOF and CoFe-MOF

95.7 mg/g after 60 min, and it took another 30 min to achieve the adsorption capacity of 100.6 mg/g. To increase the MO processing capacity, the amount of investigated material was in the range of 0.002–0.030 g/L, with other conditions being fixed. The results of Fig. 5(b) show that the adsorption capacity of both materials tends to sharply decrease when increasing the adsorbent dosage. Typically, CoFe-MOF at the concentration of 0.005 g/L has a much higher MO removal capacity (125.7 mg/g) than Fe-MOF at the concentration of 102.9 mg/g. Such an increase in MO removal efficiency may be dependent on increasing the adsorbent dosage, yet using a high dosage can reduce the diffusion capacity of the solution to the surface or change the physical properties of the material. The effect of the initial MO concentration (30–300 ppm) on the adsorption capacity was also evaluated in Fig. 5(c). The results have shown that the adsorption capacity strongly depends on the initial concentration of MO, with the highest MO removal capacity of Fe-MOF being 130.5 mg/g at the concentration of 100 ppm, while that of CoFe-MOF being 137.6 mg/g at the concentration of 200 ppm. When continuing to increase the MO concentration, the adsorption capacity decreased markedly since once the adsorption process have reached an equilibrium state, the MO residue was still high, thus filling the surface of the material. The influence of the pH factor is considered essential in the adsorption process, suggesting that the interaction between the surface of the adsorbent and the charge of the dye is an electrostatic interaction necessary for the adsorption mechanism. In addition, the size of the dye molecules (MO) is also considered a key factor in the adsorption process. The strong interaction can cause the migration of the dyes closer to the adsorbent and cause the dyes to be adsorbed rapidly. Besides, the π–π interaction of materials and aromatic rings of MO also facilitated the adsorption process [25].

In this study, the MO adsorption kinetics was evaluated based on four models of pseudo-first order and pseudo-second order. The results of the kinetic constants of both models are listed in Table 1 and Fig. 6(a). The influence of the contact time of the MO adsorption on CoFe-MOF was investigated from 0 to 240 min. According to Fig. 6(a), the equilibrium adsorption time was obtained at 60 min. Results have shown that the MO adsorption kinetics is suitable for both pseudo-first-order and pseudo-second-order models with correlation coefficients R^2 of 0.993 and 0.998, respectively. Therefore, the adsorption of MO on CoFe-MOF materials was chemisorption through the electrostatic interaction between the adsorbents.

To describe the adsorption behavior of CoFe-MOF materials, Langmuir and Freundlich's models are used to assume that the adsorption mechanism occurs on the surface of the material. Fig. 6(b) shows the effect of different concentrations (30 to 300 mg/L) on the equilibrium adsorption capacity of MO. From the study of Langmuir and Freundlich adsorption isotherm models, it can be seen that the experimental data are more consistent with the Langmuir isotherm model (Table 2). The Langmuir correlation coefficient R^2 is 0.982, which is larger than the Freundlich correlation coefficient R^2 (0.969). According to calculations from the Langmuir adsorption heat transfer equation, the maximum adsorption capacity (Q_m) is 136.19 mg/g. The results confirm that the Langmuir isotherm can be used to study the adsorption process.

Table 1. The adsorption kinetic constants

Kinetic models	Equation	Parameters	Value
Pseudo-first-order	$Q_t = Q_1 (1 - \exp(-k_1 t))$	k_1 ($min^{-1}/(mg/L)^{1/n}$)	0.21
		Q_1 (mg/g)	104.34
		R^2	0.993
Pseudo-second-order	$Qt = \frac{t}{\frac{1}{k_2 Q_2^2} + \frac{t}{Q_2}}$	$k_2 \cdot 10^4$ (g/(mg.min))	0.0054
		Q_2 (mg/g)	106.79
		R^2	0.998

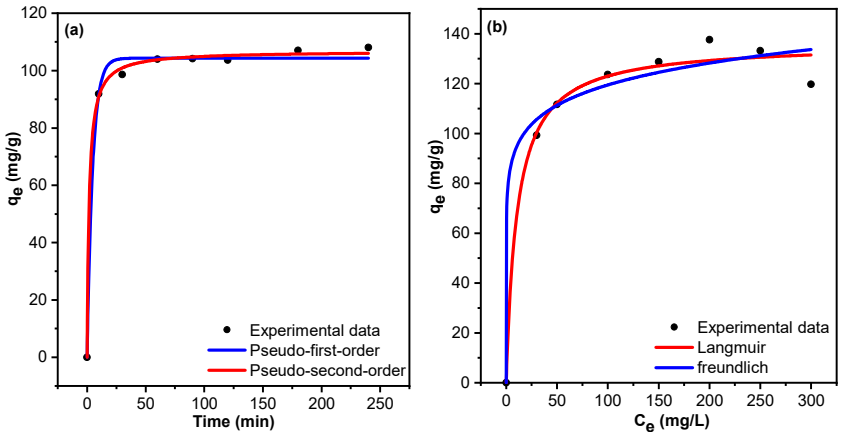

Fig 6. Kinetic and isothermal model of MO adsorption onto CoFe-MOF

Table 2. The adsorption isotherm constants

Kinetic models	Equation	Parameters	Value
Langmuir	$Q_e = \frac{Q_m K_L C_e}{1+K_L C_e}$ $R_L = \frac{1}{1+K_L C_o}$	K_L (L/mg)	0.093
		Q_m (mg/g)	136.19
		R^2	0.982
Freundlich	$Q_e = K_F C_e^{1/n}$	K_F (mg/g)/(mg/L)$^{1/n}$	74.56
		1/n	1/0.1024
		R^2	0.969

■ CONCLUSION

Fe-MOF and CoFe-MOF adsorbents were successfully synthesized at 150 °C by using the solvothermal method and DMF as the solvent. The results have shown that the CoFe-MOF material sample has a higher adsorption capacity than Fe-MOF in terms of MO removal. In acidic media (pH 4), the adsorption capacity reached 137.6 mg/g at the MO concentration of 200 ppm, the adsorbent dosage was 0.005 g/L, and the time to reach equilibrium after 60 min. The interaction between MO and CoFe-MOF dyes has been demonstrated through two kinetic models, i.e., pseudo–first order and pseudo-second order, and adsorption equilibrium data which is consistent with Langmuir isotherm with a maximum adsorption capacity of 136.19 mg/g.

■ ACKNOWLEDGMENTS

The study was supported by The Youth Incubator for Science and Technology Program, managed by Youth Development Science and Technology Center – Ho Chi Minh Communist Youth Union and Department of Science and Technology of Ho Chi Minh City with a contract number No. 10/2021/HĐ-KHCNT-VU.

■ AUTHOR CONTRIBUTIONS

Cao Phuong Khanh Phan and Vuong Thinh Ho conducted the experiment, Kim Ngan Thi Tran and Thi Nhu Dung Nguyen wrote and revised the manuscript. All authors agreed to the final version of this manuscript.

■ REFERENCES

[1] Benkhaya, S., M' rabet, S., and El Harfi, A., 2020, A review on classifications, recent synthesis and applications of textile dyes, *Inorg. Chem. Commun.*, 115, 107891.

[2] Khan, M.S., Khalid, M., and Shahid, M., 2020, What triggers dye adsorption by metal organic frameworks? The current perspectives, *Mater. Adv.*, 1 (6), 1575–1601.

[3] Khan, I., Saeed, K., Zekker, I., Zhang, B., Hendi, A.H., Ahmad, A., Ahmad, S., Zada, N., Ahmad, H., Shah, L.A., Shah, T., and Khan, I., 2022, Review on

methylene blue: Its properties, uses, toxicity and photodegradation, *Water*, 14 (2), 242.

[4] Salama, R.S., Abd El-Hakam, S., Samra, S.E., El-dafrawy, S.M., El-Hakam, S.A., Samra, S.E., El-Dafrawy, S.M., and Ahmed, A.I., 2018, Adsorption, equilibrium and kinetic studies on the removal of methyl orange dye from aqueous solution by the use of copper metal organic framework (Cu-BDC), *Int. J. Mod. Chem.*, 10 (2), 195–207.

[5] Fajriati, I., Mudasir, M., and Wahyuni, E.T., 2019, Adsorption and photodegradation of cationic and anionic dyes by TiO_2-chitosan nanocomposite, *Indones. J. Chem.*, 19 (2), 441–453.

[6] Iryani, A., Nur, H., Santoso, M., and Hartanto, D., 2020, Adsorption study of rhodamine B and methylene blue dyes with ZSM-5 directly synthesized from Bangka kaolin without organic template, *Indones. J. Chem.*, 20 (1), 130–140.

[7] Hami, H.K., Abbas, R.F., Azeez, S.A., and Mahdi, N.I., 2021, Azo dye adsorption onto cobalt oxide: Isotherm, kinetics, and error analysis studies, *Indones. J. Chem.*, 21 (5), 1148–1157.

[8] Abednatanzi, S., Gohari Derakhshandeh, P., Depauw, H., Coudert, F.X., Vrielinck, H., Van Der Voort, P., and Leus, K., 2019, Mixed-metal metal-organic frameworks, *Chem. Soc. Rev.*, 48 (9), 2535–2565.

[9] Sun, Q., Liu, M., Li, K., Han, Y., Zuo, Y., Chai, F., Song, C., Zhang, G., and Guo, X., 2017, Synthesis of Fe/M (M = Mn, Co, Ni) bimetallic metal organic frameworks and their catalytic activity for phenol degradation under mild conditions, *Inorg. Chem. Front.*, 4 (1), 144–153.

[10] Nguyen, V.H., Nguyen, T.D., Bach, L.G., Hoang, T., Bui, Q.T.P., Tran, L.D., Nguyen, C.V., Vo, D.V.N., and Do, S.T., 2018, Effective photocatalytic activity of mixed Ni/Fe-base metal-organic framework under a compact fluorescent daylight lamp, *Catalysts*, 8 (11), 487.

[11] Nguyen, H.T.T., Dinh, V.P., Phan, Q.A.N., Tran, V.A., Doan, V.D., Lee, T., and Nguyen, T.D., 2020, Bimetallic Al/Fe Metal-Organic Framework for highly efficient photo-Fenton degradation of rhodamine B under visible light irradiation, *Mater. Lett.*, 279, 128482.

[12] Tang, J., and Wang, J., 2020, Iron-copper bimetallic metal-organic frameworks for efficient Fenton-like degradation of sulfamethoxazole under mild conditions, *Chemosphere*, 241, 125002.

[13] Choi, S., Cha, W., Ji, H., Kim, D., Lee, H.J., and Oh, M., 2016, Synthesis of hybrid metal-organic frameworks of $\{Fe_xM_yM'_{1-x-y}\}$-MIL-88B and the use of anions to control their structural features, *Nanoscale*, 8 (37), 16743–16751.

[14] Dey, C., Kundu, T., Biswal, B.P., Mallick, A., and Banerjee, R., 2014, Crystalline metal-Organic frameworks (MOFs): Synthesis, structure and function, *Acta Crystallogr., Sect. B: Struct. Sci., Cryst. Eng. Mater.*, 70 (1), 3–10.

[15] Soni, S., Bajpai, P.K., Mittal, J., and Arora, C., 2020, Utilisation of cobalt doped Iron based MOF for enhanced removal and recovery of methylene blue dye from waste water, *J. Mol. Liq.*, 314, 113642.

[16] Nguyen, H.T.T., Tran, K.N.T., Van Tan, L., Tran, V.A., Doan, V.D., Lee, T., and Nguyen, T.D., 2021, Microwave-assisted solvothermal synthesis of bimetallic metal-organic framework for efficient photodegradation of organic dyes, *Mater. Chem. Phys.*, 272, 125040.

[17] Wang, M., Yang, L., Guo, C., Liu, X., He, L., Song, Y., Zhang, Q., Qu, X., Zhang, H., Zhang, Z., and Fang, S., 2018, Bimetallic Fe/Ti-based metal–organic framework for persulfate-assisted visible light photocatalytic degradation of Orange II, *ChemistrySelect*, 3 (13), 3664–3674.

[18] Ding, L., Zeng, M., Wang, H., and Jiang, X.B., 2021, Synthesis of MIL-101-derived bimetal–organic framework and applications for lithium-ion batteries, *J. Mater. Sci.: Mater. Electron.*, 32 (2), 1778–1786.

[19] Blake, A.B., Yavari, A., Hatfield, W.E., and Sethulekshmi, C.N., 1985, Magnetic and spectroscopic properties of some heterotrinuclear basic acetates of chromium(III), iron(III), and divalent metal ions, *J. Chem. Soc., Dalton Trans.*, 12, 2509–2520.

[20] Cheng, X., Zhang, A., Hou, K., Liu, M., Wang, Y., Song, C., Zhang, G., and Guo, X., 2013, Size- and morphology-controlled NH_2-MIL-53(Al) prepared

in DMF–water mixed solvents, *Dalton Trans.*, 42 (37), 13698–13705.

[21] Liang, H., Liu, R., Hu, C., An, X., Zhang, X., Liu, H., and Qu, J., 2021, Synergistic effect of dual sites on bimetal-organic frameworks for highly efficient peroxide activation, *J. Hazard. Mater.*, 406, 124692.

[22] Wu, Q., Siddique, M.S., and Yu, W., 2021, Iron-nickel bimetallic metal-organic frameworks as bifunctional Fenton-like catalysts for enhanced adsorption and degradation of organic contaminants under visible light: Kinetics and mechanistic studies, *J. Hazard. Mater*, 401, 123261.

[23] Wang, Z., Wu, C., Zhang, Z., Chen, Y., Deng, W., and Chen, W., 2021, Bimetallic Fe/Co-MOFs for tetracycline elimination, *J. Mater. Sci.*, 56 (28), 15684–15697.

[24] Shakly, M., Saad, L., Seliem, M.K., Bonilla-Petriciolet, A., and Shehata, N., 2022, New insights into the selective adsorption mechanism of cationic and anionic dyes using MIL-101(Fe) metal-organic framework: Modeling and interpretation of physicochemical parameters, *J. Contam. Hydrol.*, 247, 103977.

[25] Valadi, F.M., Ekramipooya, A., and Gholami, M.R., 2020, Selective separation of Congo Red from a mixture of anionic and cationic dyes using magnetic-MOF: Experimental and DFT study, *J. Mol. Liq.*, 318, 114051.